Dimensionality influence on passive scalar transport.

M.Iovieno, L.Ducasse, D.Tordella

Dipartimento di Ingegneria Aeronautica e Spaziale, Politecnico di Torino, Italy

E-mail: michele.iovieno@polito.it

Abstract. We numerically investigate the advection of a passive scalar through an interface placed inside a decaying shearless turbulent mixing layer. We consider the system in both two and three dimensions. The dimensionality produces a different time scaling of the diffusion, which is faster in the two-dimensional case. Two intermittent fronts are generated at the margins of the mixing layer. During the decay these fronts present a sort of propagation in both the direction of the scalar flow and the opposite direction. In two dimensions, the propagation of the fronts exhibits a significant asymmetry with respect to the initial position of the interface and is deeper for the front merged in the high energy side of the mixing. In three dimensions, the two fronts remain nearly symmetrically placed. Results concerning the scalar spectra exponents are also presented.

1. Introduction

The advection of a passive substance by a turbulent flow is important in many natural and engineering contexts, e.g. turbulent mixing, combustion, pollution dispersal, in which the prediction of mixing and dispersion rates of a scalar contaminant is a problem of great interest because of the concern over the design of efficient mixing and combustion devices and over environmental emissions. Although the concentration of such a passive substance exhibits a complex behaviour that shows many phenomenological parallels with the behaviour of the turbulent velocity field, the statistical properties of 'passive scalar' turbulence, strongly influenced by the Kolmogorov cascade phenomenology, are in part decoupled from those of the underlying velocity field, Shraiman & Siggia (2000). The subject, in the last years, is in fact undergoing a reinterpretation as empirical evidence shows that local isotropy, both at the inertial and dissipation scales, is violated (Warhaft (2000)). Moreover, in practice, dispersion usually occurs in time dependent inhomogeneous flows, which present a much more complicate behaviour than homogeneous flows and thus are beyond the reach of analytical models or even numerical simulations. In this work, we go one step beyond the homogeneous and isotropic turbulence and consider the simplest inhomogeneous and shearfree turbulent Navier-Stokes motion: the system where one energetic turbulent isotropic field is left to convectively diffuse into a low energy one. In this system the region where the two turbulences interact is preceded by a highly intermittent thin layer - where the energy flux is maximum - that propagates into the low energy region, see Tordella & Iovieno (2006); Tordella *et al.* (2008). The presence of the interaction zone offers the way to carry out numerical measurements of the long-term temporal turbulent diffusivity in an inhomogeneous flow.

The initial condition construction and computational methoid are described in section 2. In section 3, we present new results concerning the passive scalar turbulent transport in two and

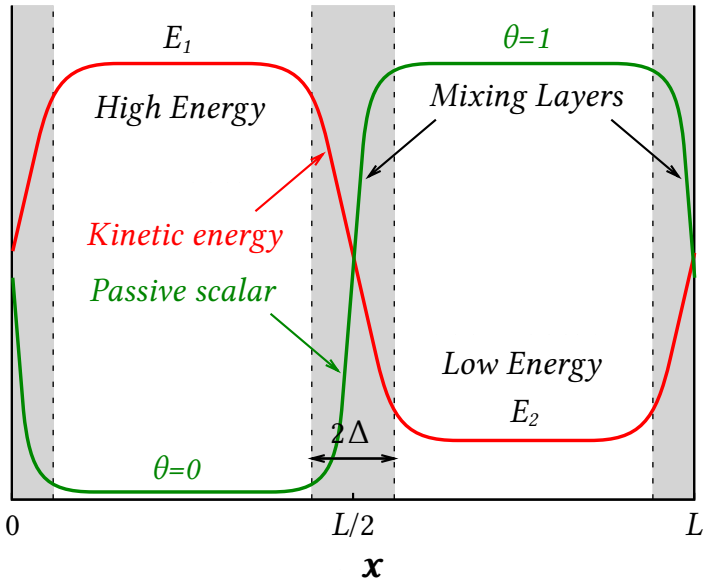

Figure 1. Scheme of the flow. Due to the use of periodic boundary conditions, two mixing layers are included in the computational domain along the x direction, which is the direction where the nonhomogeneoity tkes places. The flow is homogeneous in the other two direction,s y_1 and y_2, not shown in the sketch. L is the domain size in x direction, equal to 2π in two dimensions and 4π in three dimensions. As a reference dimensional field, we considered the following set of data: $L = 41$ cm, $E_1 = 8.2$ J/kg. The initial conditions for the velocity are generated by a linear matching of two homogeneous and isotropic fields over a thickness Δ, see equation (1), while the initial mean scalar distribution is a discontinuity smoothed enough to avoid the Gibbs phenomenon, see equation (2).

three dimensions, which comprehend the first four moments of the scalar concentration, the skewness and kurtosis of the scalar derivative and the scalar spectra.

2. Method

Figure 1 shows a schematic diagram of the flow configuration and the coordinate system used: the two isotropic fields are initially separated by a layer which is as thick as the correlation length ℓ. From a numerical point of view, the flow is assumed to be contained in a parallelepiped (or a rectangle in two dimensions) and periodic boundary conditions are applied to all the spatial directions. The coordinate system is chosen with the x axis along the direction of the energy gradient, axis y_1 and y_2 along the homogeneous directions. The initial condition is obtained by matching two homogeneous and isotropic fields with the same integral scale but with a different turbulent kinetic energy. In practice, the initial condition is generated as $u_i = u_i^{(1)} p(x)^{\frac{1}{2}} + u_i^{(2)} (1 - p(x))^{\frac{1}{2}}$, where $u_i^{(1)}$ and $u_i^{(2)}$ are the velocity of two homogeneous and isotropic fields with turbulent kinetic energies equal to E_1 and E_2. Function $p(x)$, defined as

$$p(x) = \frac{1}{2}\left[1 + \tanh a\frac{x}{L} \tanh a\frac{x - L/2}{L} \tanh a\frac{x - L}{L}\right] \tag{1}$$

is the weighting function which allows a smooth transition, L is the domain size in the x direction and a is a constant, which is chosen in order to have an initial transition layer that is no larger

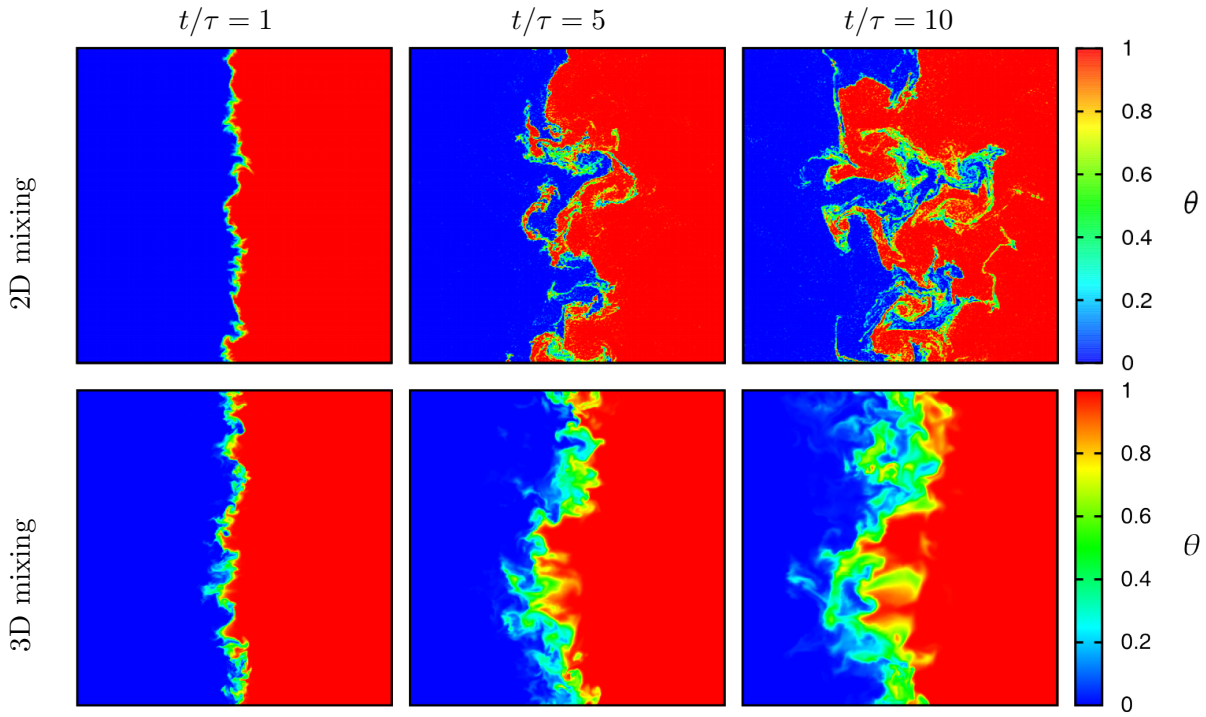

Figure 2. Visualization of the scalar field in the central part of the computational domain. The high turbulent energy velocity field is on the left of each image. The three different instants correspond, from left to right, to $t/\tau = 1, 5, 10$, respectively. τ is the initial eddy turnover time of the high energy region. The three-dimensional simulation has an initial R_λ equal to 150 in the high energy isotropic region and 60 in the low energy region.

than the integral scale ($a = 55$). In this study, $u_i^{(2)} = u_i^{(1)}/\mathcal{E}^{1/2}$, where $\mathcal{E} = E_1/E_2$ is the imposed initial energy ratio and the two regions have the same integral scale. A description of the possible enhancement or damping of the turbulent diffusion and interace penetration associated to the presence of different integral scale can be found in Tordella & Iovieno (2006).

In order to analyse the diffusion of the passive scalar interface across the kinetic energy mixing layer, the passive scalar is introduced in the low energy region of the flow at $t = 0$. To avoid the Gibbs phenomenon, the discontinuity is replaced by a sufficiently smooth transition. The initial condition for the passive scalar θ is thus defined as

$$\theta(x, y_i) = \frac{1}{2}\left[1 - \tanh 2a\frac{x}{L}\tanh 2a\frac{x - L/2}{L}\tanh 2a\frac{x - L}{L}\right], \tag{2}$$

with $a = 55$. No scalar fluctuation is introduced: the scalar concentration is initially uniform in the two isotropic regions, $\theta = 0$ in the high energy region and $\theta = 1$ in the low energy region. Scalar variance will be generated by the underlying turbulent flow, see figure 2. The Schmidt number is assumed to be equal to one in all the simulations.

In the three-dimensional simulations, the turbulent field $u_i^{(1)}$ has a Taylor microscale Reynolds number equal to 150. Directions y_1 and y_2 in this flow configuration remain statistically homogeneous during the decay, so that all the statistics can be computed as plane averages in these directions.

The mass, momentum and and the scalar transport equation are solved by using a dealiased pseudospectral Fourier-Galerkin spatial discretization coupled with a fourth order Runge-Kutta

explicit time integration. In the two dimensional simulations the diffusive terms $\nabla^2 u_i/Re$ and $\nabla^2\theta/(ReSc)$ have been replaced by artificial hyper-viscosity terms proportional to $-\nabla^4 u_i$ and $-\nabla^4\theta$. Hyper-viscosity is used to concentrate the influence of diffusion terms at the highest wavenumbers and to extend the intertial range. The size of the computational domain is $4\pi \times (2\pi)^2$ (discretized with 1200×600^2 grid points) in the three-dimensional simulations and $(2\pi)^2$ (discretized with 1024^2 grid points) in the two-dimensional simulations. For details on the numerical technique and initial conditions generation, see Iovieno *et al.* (2001); Tordella & Iovieno (2006); Tordella *et al.* (2010).

We have carried out a numerical experiments with an imposed initial energy ratio of 6.7 in both two and three dimensions. About 22 initial eddy turnover times have been simulated in two dimensions and 12.5 initial eddy turnover times in three dimensions. It has been extimated that, due to the mixing layer growth, the two separate homogeneous and isotropic regions will be destroyed after after about 30-35 initial eddy turnover times.

3. Results and discussion

The initial conditions produce a kinetic energy gradient in the direction of inhomogeneity (x). Outside this inhomogeneous region, the kinetic energy in the two turbulence fields decays as a power law, with exponent approximately equal to -1.2, in the three-dimensional simulations, while in two dimensions there is no significant energy decay. In both cases, the initially imposed energy ratio is preserved during the time evolution of the flow.

In all flow configurations, the mixing layer was observed to be highly intermittent and the velocity fluctuations in the x direction have large skewness and kurtosis, see Veeravalli & Warhaft (1989); Tordella & Iovieno (2006); Tordella *et al.* (2008). Across the mixing the second, third and fourth velocity moments collapse using a single lenghtscale, the mixing width Δ_E, conventionally defined as the distance between the points with normalized energy $(E(x,t) - E_2(t))/(E_1(t) - E_2(t))$ equal to 0.75 and 0.25. In this paper, we focus on the scalar dispersion through the shearless mixing layer.

A visualization of the time evolution of the scalar concentration at three different instants is shown in figure 2. The scalar interface, which initially separates the low energy region with scalar concentration $\theta = 1$ (on the right of the figures) from the high energy region with scalar concentration $\theta = 0$, is spread by turbulent eddies and a scalar mixing region with high scalar variance is generated. The width of this region can be measured by considering the mean scalar distributions (figure 3). The scalar mixing layer thickness Δ_θ is defined, in analogy with the energy layer thickness Δ_E, as the distance between the points with means scalar $\overline{\theta}$ equal to 0.75 and 0.25. After an initial transient of about one eddy-turnover time, the time evolutions of these interaction widths follow those observed for the self-diffusion of the velocity field with the same dimensionality, and a stage of evolution with a power law scaling of the mixing thickness is reached in both two and three dimensions. However, the time scaling of the growth of the interaction width is superdiffusive in two dimensions ($\Delta_\theta \sim t^{0.68}$), while it is very slightly subdiffusive in three dimensions ($\Delta_\theta \sim t^{0.46}$), see figure 3. The scalar flux $\overline{\theta' u'}$ is consequently always higher in two dimensions (figure 3(b, d)). Therefore, scalar diffusion in two dimensions is asymptotically faster than in three dimensions, a result already observed in the kinetic energy mixing (see Tordella *et al.* (2010)). In three dimensions there is a fair agreement with the wind tunnel experiments on the scalar diffusion from a linear source in a shearless mixing (Veeravalli & Warhaft (1989, 1990)).

A mixed region with high variance is immediately generated in the centre of the interaction layer. In the three-dimensional flow, the scalar variance has already reached its maximum after less than one eddy turnover time and, since that instant, it slowly decreases. In the following 10 eddy turnover times, about 20% of the variance ar $t/\tau = 1$ is lost. In two dimensions, the scalar

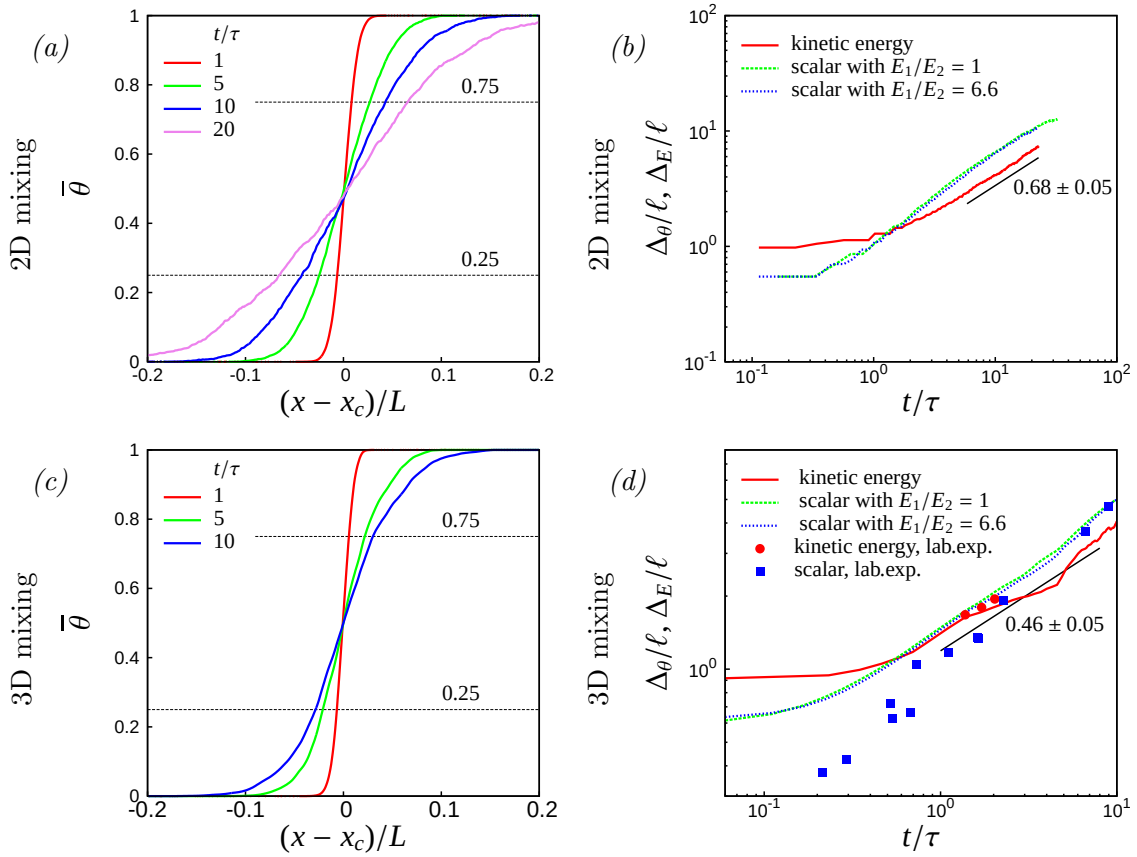

Figure 3. Left (a-c): mean scalar profiles in the simulations with initial energy ratio $E_1/E_2 = 6.7$, L is the domain size in the x direction and x_c the centre of the mixing layer. The dashed horizontal lines indicates $\overline{\theta} = 0.25$ and $\overline{\theta} = 0.75$. Right (b-d): Interaction layer thickness, normalized with the initial integral scale ℓ. The scalar layer thickness Δ_θ is defined as the distance between the points where $\overline{\theta}$ is equal to 0.25 and 0.75. The energy layer thickness is defined as the distance between the points where the normalized turbulent kinetic energy $(E - E_2)/(E_1 - E_2)$ is equal to 0.25 and 0.75 as in Tordella *et al.* (2008). The exponents of the power law fitting of the scalar thickness growth are indicated. The accuracy of the exponents is about 10%. The same mixing length growth can be observed in the absence of the kinetic energy gradient ($E_1/E_2 = 1$). Experimental data are from the wind tunnel experiments by Veeravalli & Warhaft (1989) and Veeravalli & Warhaft (1990) with $E_1/E_2 = 7$. It should be noted that in this last work the authors propose an exponent of 0.34 for the final stage of the scalar dispersion.

flow is almost twice as large and the initial variance generation last longer: the maximum is attained later and is about 50% higher. Notwithstanding the presence of the energy gradient, the mean scalar and scalar variance profiles are almost symmetric, see figures 3 and 4. The presence of the turbulent energy gradient is instead felt on the distribution of higher order moments as the scalar skewness and kurtosis shown in figures 5.

In contrast with the velocity field, the spatial distribution of these moments show the presence of two intermittent fronts at the borders of the mixed region. In the three dimensional case, these fronts are both at a distance from the mixing centre approximatively equal to $2\Delta_\theta$. The asymmetry in their position and in their intermittency levels is mild and tend to be less pronounced as the mixing proceeds. On the contrary, in two dimensions the front toward the high energy regions penetrates much more than the one toward the low energy region. After about 5 initial eddy turnover times the depth of penetration is about $2\Delta_\theta$ in the high energy

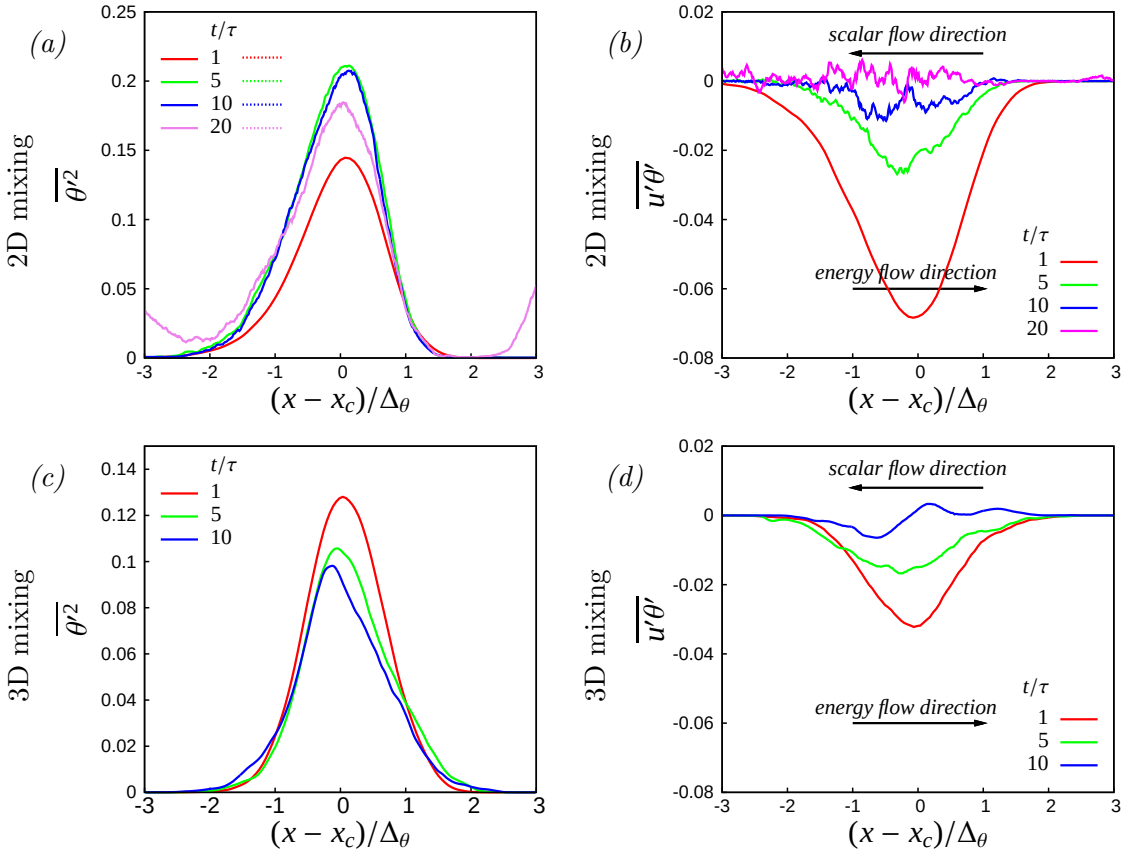

Figure 4. Left (a-c): Scalar variance in the simulations with initial energy ratio $E_1/E_2 = 6.7$. Right (b-d): scalar flow $\overline{u'\theta'}$ in the simulations with initial energy ratio $E_1/E_2 = 6.7$. The arrows indicate the scalar and energy flow directions.

region and about Δ_θ in the low energy region, see figure 5.

Because of the gradual thickening of the mixing layer, the kinetic energy and the scalar gradients, which drive the scalar spreading, become milder and milder. As a consequence, not only the scalar flux is reduced, see figure 3(b, d), but also the intermittency levels of the two scalar fronts decrease in time, even if in a slower fashion. Because of the energy decay, this reduction is faster in three dimensions: the peaks in the distributions of skewness and kurtosis present the same levels in two and three dimensions after about one eddy turnover times but, after ten eddy turnover times, the peaks of skewness and kurtosis are twice as high in the two dimensional mixing.

Intermittency is not limited to large scale scalar fluctuations, but is quickly spread to small scale fluctuations, as can be inferred from the skewness and kurtosis of the scalar derivative in the inhomogeneous direction x, which are shown in figure 6. Two peaks of large intermittency can be seen in correspondence of the two intermittent fronts since $t/\tau = 1$. However, their time evolution is different from the one seen for large scale scalar fluctuations: the peaks tend to decay in time, but small scale intermittency tends to last longer in the three dimensional case. In two dimensions, the peak of the derivative skewness in the front facing the high energy region is almost vanished after ten eddy turnover times while the one in the front facing the low energy side is about half the one present in the three dimensional case.

Simulations in absence of an energy gradient (i.e., $E_1/E_2 = 1$), not shown in the figures, exhibit the same mixing lenght temporal growth but the two scalar intermittent fronts at the

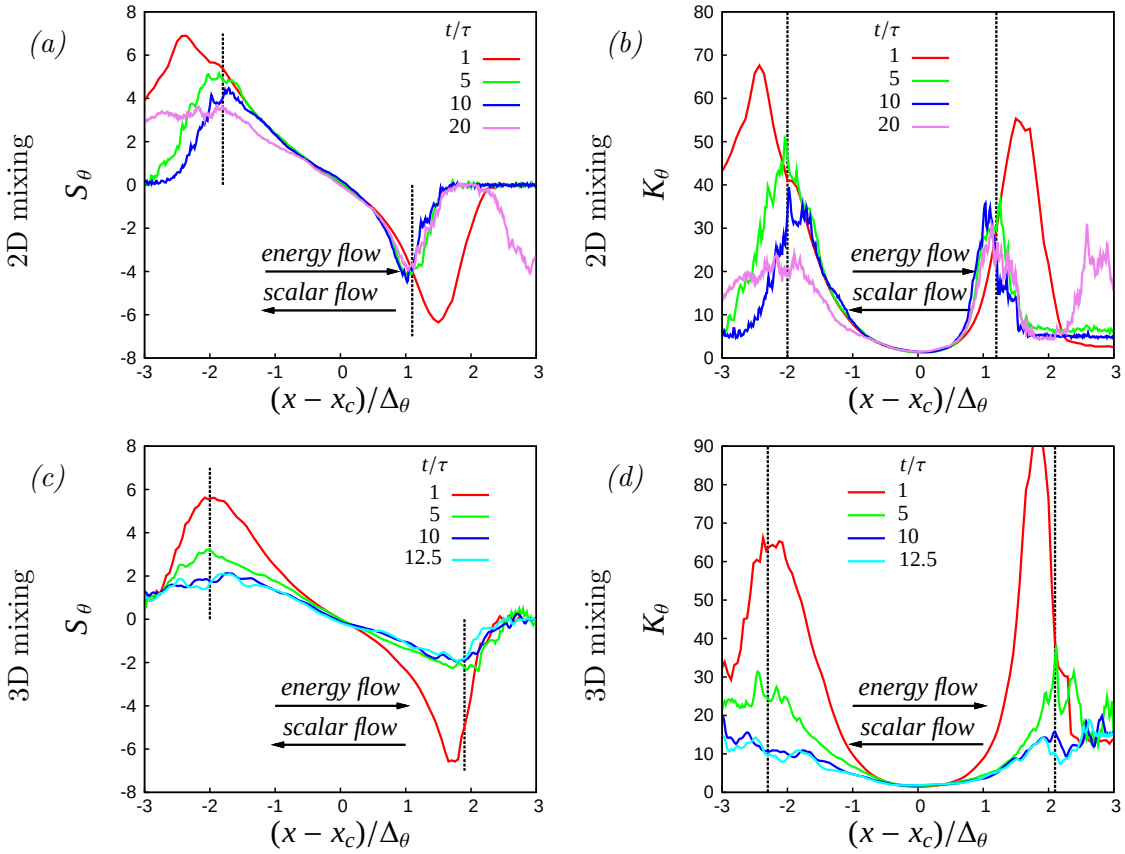

Figure 5. Left (a-c): Scalar skewness distribution in the simulations with initial energy ratio $E_1/E_2 = 6.7$. Right (b-d): scalar kurtosis distributions in the simulations with initial energy ratio $E_1/E_2 = 6.7$. The vertical dashed lines indicate the position of maximum intermittence at the end of the simulation. The arrows indicate the scalar and energy flow directions which are opposite in this simulations. Leaving aside the sign, the distributions remain unchanged when the passive scalar mean gradient is concurrent with the energy gradient.

borders of the mixing layer become symmetric.

In the central part of the mixing layer, between the two intermittent fronts, the scalar fluctuations tend, after few eddy turnover times, to an almost steady state. The variance decays very slowly (even in the three-dimensional flow, which has a relevant kinetic energy decay of the underlying flow), see figure 4(a,c), and the one-dimensional spectra show a full range of scales. In figure 7, one-dimensional passive scalar and velocity spectra are shown. The spectra have been compensated by their inertial range exponents. In two dimensions, the passive scalar exponent in the inertial range is about -1.4, which is roughly one half of the -3 exponent of the velocity field and is far from the κ^{-1} inertial range scaling of homogeneous and statistically stationary flows (see, e.g., Bos *et al.* (2009)). In three dimensions, the difference between scalar and velocity exponents is very mild and both tend to approach the homogeneous turbulence scaling. However, the scalar spectrum seems to show a wider inertial range region, a feature which has been observed also in homogeneous flows at moderate Reynolds numbers, see Danaila & Antonia (2009).

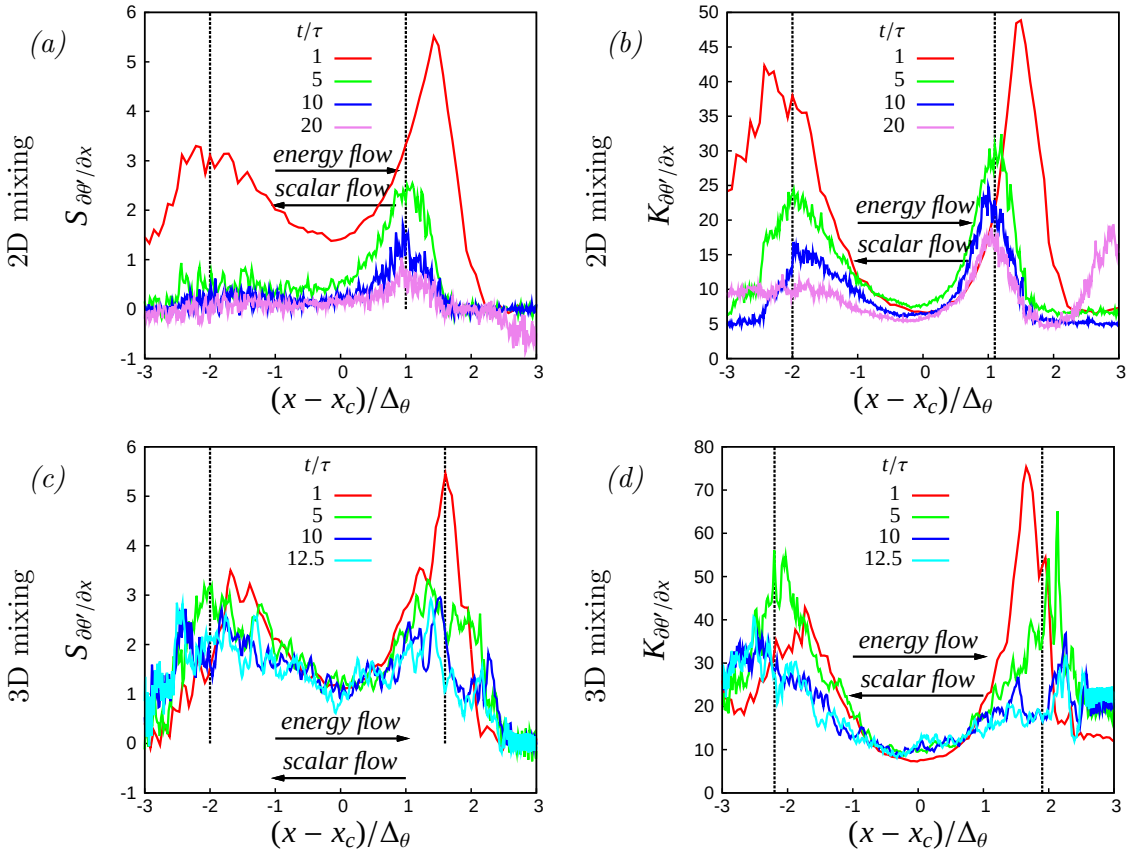

Figure 6. Skewness (a-c) and kurtosis (b-d) distributions of the derivative of the scalar fluctuation in the inhomogeneous direction x, simulations with initial energy ratio $E_1/E_2 = 6.7$. The skewness changes sign when the passive scalar is introduced in the high energy region (left) instead of in the low energy region (right).

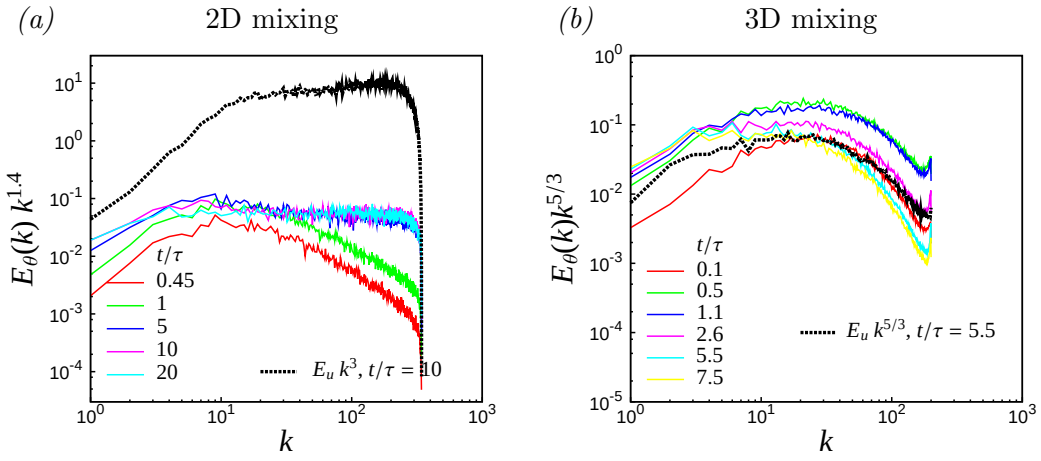

Figure 7. Compensated scalar one-dimensional spectra in the centre of the mixing layer in two (part a) and three dimensions (part b). The black dashed lines reproduce, at one instant, the compensated one-dimensional velocity spectrum in the same position. All spectra have been computed by integrating over the homogeneous directions y_i.

4. Conclusions

The diffusion length, Δ_θ, of a passive scalar through a shearless turbulent mixing follows closely the temporal evolution of the self-diffusion length, Δ_E, of the velocity field. In two dimensions the growth is faster: $\Delta_E \sim \Delta_\theta \sim t^{0.68}$, while in three dimensions $\Delta_E \sim \Delta_\theta \sim t^{0.46}$. The scalar flow is about two times larger in two dimensions than in three dimensions. Also the scalar variance in the centre of the mixed layer is 50% higher in two dimensional case.

An important observation concerns the presence of two scalar intermittent fronts which appear at the sides of the mixed region. The intermittency levels of the fronts is high and gradually decay in time. In all simulations, the fronts move from the initial position of the interface. That on the high energy side of the mixing penetrates deeper into it. This asymmetry is milder in the three-dimensional case. The intermittency is not limited to the large scale, but involves also the small scale. In two dimensions, the small scale intermittency decay is very fast. In three dimensions, it is more intense and lasts longer. The large scale intermittency follows an opposite behaviour.

In the centre of the mixing layer, in three dimensions, the passive scalar and velocity spectra both show an inertial range with an exponent close to -5/3. In two dimensions, the velocity shows a κ^{-3} inertial range, while the passive scalar shows a $\kappa^{-1.4}$ inertial range. An exponent value which is closer to the three dimensional $\kappa^{-5/3}$ scaling than to the two dimensional k^{-1} scaling, which is observed in the case of passive scalar transport in homogeneous condition.

Acknowledgements

The authors would like to thank CINECA computing centre (`http://www.cineca.it`) for supporting this work.

References

Bos, W. J., Kadoch, B., Schneider, K. & Bertoglio, J. P. 2009 Inertial range scaling of the scalar flux spectrum in two-dimensional turbulence. *Phys. Fluids* **21**, 115105/1–8.

Danaila, L. & Antonia, R. A. 2009 Spectrum of a passive scalar in moderate Reynolds number homogeneous isotropic turbulence. *Phys. Fluids.* **21**, 111702/1–4.

Iovieno, M., Cavazzoni, C. & Tordella, D. 2001 A new technique for a parallel dealiased pseudospectral Navier-Stokes code. *Comp. Phys. Comm.* **141**, 365–374.

Shraiman, B. I. & Siggia, B. I. 2000 Scalar turbulence. *Nature* **405**, 639–646.

Tordella, D. & Iovieno, M. 2006 Numerical experiments on the intermediate asymptotics of the shear-free turbulent transport and diffusion. *J. Fluid Mech.* **549**, 429–441.

Tordella, D., Iovieno, M. & Bailey, P. R. 2008 Sufficient condition for gaussian departure in turbulence. *Phys. Rev. E* **77**, 016309/1–11.

Tordella, D., Iovieno, M. & Ducasse, L. 2010 Passive scalar diffusion through a turbulent energy gradient. EFMC-10, Bad Reichenhall.

Veeravalli, S. & Warhaft, Z. 1989 The shearless turbulence mixing layer. *J. Fluid Mech.* **207**, 191–229.

Veeravalli, S. & Warhaft, Z. 1990 Thermal dispersion from a line source in the shearless turbulence mixing layer. *J. Fluid Mech.* **216**, 35–70.

Warhaft, Z. 2000 Passive scalar in turbulent flows. *Ann. Rev. Fluid Mech.* **32**, 203–240.